



Near-infrared photoimmunotherapy in the models of hepatocellular carcinomas using cetuximab-IR700

Seiichiro Takao | Hiroshi Fukushima | A. Paden King | Takuya Kato | Aki Furusawa  |
Shuhei Okuyama | Makoto Kano | Peter L. Choyke | Freddy E. Escorcía |
Hisataka Kobayashi 

Molecular Imaging Branch, Center for Cancer Research, National Cancer Institute, NIH, Bethesda, Maryland, USA

Correspondence

Hisataka Kobayashi, Molecular Imaging Branch, Center for Cancer Research, National Cancer Institute, NIH, 10 Center Drive, Bethesda 20892, MD, USA.
Email: kobayash@mail.nih.gov

Funding information

National Cancer Institute, Grant/Award Number: ZIA BC011513

Abstract

Epidermal growth factor receptor (EGFR) has emerged as an important therapeutic target in many cancers, and overexpression of EGFR is frequently observed in hepatocellular carcinomas (HCCs). Near-infrared photoimmunotherapy (NIR-PIT) is a new anticancer treatment that selectively damages the cell membrane of cancer cells after NIR light-induced photochemical reaction of IR700, which is bound to a targeting antibody on the cell membrane. NIR-PIT using cetuximab-IR700 has already been approved in Japan, is under review by the US Food and Drug Administration (FDA) for advanced head and neck cancers, and its safety has been established. However, EGFR has not been investigated as a target in NIR-PIT in HCCs. Here, we investigate the application of NIR-PIT using cetuximab-IR700 to HCCs using xenograft mouse models of EGFR-expressing HCC cell lines, Hep3B, HuH-7, and SNU-449. In vitro NIR-PIT using EGFR-targeted cetuximab-IR700 killed cells in a NIR light dose-dependent manner. In vivo NIR-PIT resulted in a delayed growth compared with untreated controls. In addition, in vivo NIR-PIT in both models showed histological signs of cancer cell damage, such as cytoplasmic vacuolation and nuclear dysmorphism. A significant decrease in Ki-67 positivity was also observed after NIR-PIT, indicating decreased cancer cell proliferation. This study suggests that NIR-PIT using cetuximab-IR700 has potential for the treatment of EGFR-expressing HCCs.

KEYWORDS

cancer, epidermal growth factor receptor, hepatocellular carcinoma, Ki-67 antigen, near-infrared photoimmunotherapy

Abbreviations: APC, antibody-photoabsorber conjugate; DIC, differential interference contrast; DIG, digoxigenin; EGFR, epidermal growth factor receptor; HCC, hepatocellular carcinoma; IR700, IRDye700DX; LDT, liver-directed therapy; mAb, monoclonal antibody; NIR-PIT, near-infrared photoimmunotherapy; RFI, relative fluorescence intensity.

This is an open access article under the terms of the [Creative Commons Attribution-NonCommercial](https://creativecommons.org/licenses/by-nc/4.0/) License, which permits use, distribution and reproduction in any medium, provided the original work is properly cited and is not used for commercial purposes.

Published 2023. This article is a U.S. Government work and is in the public domain in the USA. *Cancer Science* published by John Wiley & Sons Australia, Ltd on behalf of Japanese Cancer Association.

1 | INTRODUCTION

Hepatocellular carcinoma (HCC) is the most common type of primary liver cancer, which is the sixth most-diagnosed cancer, and it was the third leading cause of cancer death worldwide in 2020.¹ HCC typically develops in the setting of chronic liver inflammation and cirrhosis.² Therefore, it is critical to consider two clinical features when selecting liver-directed therapies (LDTs). First, it is crucial to kill hepatic cancer cells while minimizing damage to the already impaired liver. Secondly, due to chronic inflammation, there is a propensity for the development of new HCCs following the treatment of the lesion. Therefore, it is desirable that therapies be repeatable without further decreasing liver reserve in a patient with already compromised liver function.³ Thus, due to factors beyond disease stage, the treatment options for HCC are frequently constrained, leading to ongoing development of novel therapeutic approaches.

Near-infrared photoimmunotherapy (NIR-PIT) is a newly developed cancer therapy using an antibody–photoabsorber conjugate (APC) that is highly selective for tumor.^{4,5} APCs are created by conjugating the photoabsorber IRDye700Dx (IR700), a silica-phthalocyanine dye, to a monoclonal antibody (mAb) that target antigens on the surface of cancer cells.⁵ After intravenous infusion of APCs, APCs bind to cancer cells generally within 24 h in humans. Upon the local application of NIR light, the APC changes from hydrophilic to markedly hydrophobic, as the axial ligands of IR700 dissociate from the remainder of the molecule.⁶ This process causes aggregation of APCs and cell surface antigens that are bound to them, ultimately resulting in substantial and irreversible cellular membrane damage. Cancer cells rapidly undergo swelling, blebbing, and rupture, leading to selective eradication of cancer cells while releasing highly immunogenic cellular contents into the tumor microenvironment.⁷ This process is known as immunogenic cell death (ICD), which activates the host immune system against antigens released from killed cancer cells.⁵ Cancer immunotherapy is emerging as a pivotal therapy in the strategy of HCC, which has a metachronous and multicentric incidence. Moreover, NIR light is intrinsically harmless to normal cells that do not bind the APC. Therefore, NIR-PIT has the potential to be an ideal therapy for HCC from the perspective of killing current HCC cells, preventing recurrence of HCC while preserving residual liver function.

Human epidermal growth factor receptor (EGFR) is a transmembrane receptor that belongs to the ErbB family of receptor tyrosine kinases. It is known to be overexpressed in many types of cancer, including HCC,^{8,9} making it an attractive target for NIR-PIT.¹⁰ The overexpression of EGFR and the EGFR signaling pathway correlates with a more aggressive disease, as indicated by clinical signs such as intrahepatic metastases, tumor size, and pathologic signs such as high proliferation index and dedifferentiation.^{9,11–13} EGFR activation in HCC confers resistance to kinase inhibitors, and EGFR-targeted therapies in HCC have yielded unsatisfactory outcomes so far.^{14–16} However, NIR-PIT is unaffected by resistance mechanisms such as mutations in the extracellular domain of EGFR as long as EGFR is overexpressed on the cell membrane surface. EGFR-targeted

NIR-PIT is currently in phase III clinical testing for locoregional recurrent head and neck squamous cell carcinoma in patients who have failed at least two lines of therapy (LUZERA-301, NCT03769506). Cetuximab-IR700 conjugate (Akalux™, Rakuten Medical Inc.) has already been approved for clinical use by the Pharmaceuticals and Medical Devices Agency in Japan in September 2020, having demonstrated both efficacy and safety for human use. Other EGFR-expressing tumors may also benefit from NIR-PIT. The purpose of this study is to investigate the potential application of NIR-PIT using cetuximab-IR700 in the treatment of HCC.

2 | MATERIALS AND METHODS

2.1 | Reagents

Water-soluble silica-phthalocyanine derivative IRDye700DX NHS ester ($C_{74}H_96N_{12}Na_4O_{27}S_6Si_3$; molecular weight of 1954.22) was obtained from LI-COR Bioscience. Cetuximab, a chimeric (mouse/human) mAb directed against EGFR, was purchased from Bristol-Meyers Squibb Co.

2.2 | Synthesis of IR-700-conjugated cetuximab (Cet-IR700)

Conjugation of IR700 with mAb has been previously described.¹⁷ Briefly, cetuximab (1 mg, 6.6 nmol) was incubated with IR700 NHS ester (66.8 μ g, 34.2 nmol, 5 mmol/L in DMSO) in 0.1 mol/L Na_2HPO_4 (pH 8.5) at room temperature for 1 h. The mixture was purified with a Sephadex G50 column (PD-10; Cytiva). The protein concentration was determined with the Coomassie Plus protein assay kit (Thermo Fisher Scientific Inc.) by measuring the absorption at 595 nm with spectroscopy (8453 Value System; Agilent Technologies). A concentration of IR700 was measured by absorption at 689 nm with spectroscopy to confirm the number of fluorophore molecules conjugated to each mAb. The synthesis was controlled so that an average of three IR700 molecules were bound to a single antibody.

2.3 | Cell lines and culture

Hep3B and SNU-449 HCC cell lines, and Ramos, Epstein-Barr virus-negative B-cell lymphoma cell lines were purchased from the American Type Culture Collection (ATCC). HuH-7 cells were purchased from Riken. Hep3B and HuH-7 were grown in Dulbecco's modified minimum essential medium (DMEM; ATCC) supplemented with 10% fetal calf serum and penicillin (100 unit/mL)/streptomycin (100 μ g/mL; Life Technologies) in tissue culture flasks in a humidified incubator at 37°C at an atmosphere of 95% air and 5% carbon dioxide. SNU-449 and Ramos were grown in RPMI 1640 (Life Technologies) supplemented with 10% fetal bovine serum and penicillin (100 unit/mL)/streptomycin (100 μ g/mL; Life Technologies) in tissue culture

flasks in a humidified incubator at 37°C at an atmosphere of 95% air and 5% carbon dioxide.

2.4 | In vitro EGFR expression analysis

To assess in vitro EGFR expression on Hep3B, HuH-7, SNU-449, or Ramos cells, 2×10^5 cells were collected in 100 μ L PBS and incubated with PE-labeled anti-EGFR Ab (clone D1D4J; Cell Signaling Technology) or its PE-labeled Rabbit IgG isotype control (polyclonal; Cell Signaling Technology) as well as Fixable Viability Dye (Thermo Fisher Scientific), which can detect compromised cell membranes for 30 min at 4°C. After washing with PBS, the fluorescence of the cells was analyzed by BD FACSLyric (BD Biosciences) and FlowJo software (BD Biosciences). Relative fluorescence intensity (RFI) was defined as the ratio of specific fluorescence (mean fluorescence of target cells incubated with the PE-labeled anti-EGFR Ab) over nonspecific fluorescence (mean fluorescence of target cells incubated with the PE-labeled Rabbit IgG isotype control).

2.5 | In vitro cell-specific binding analysis

To verify the in vitro binding of Cet-IR700 to Hep3B, HuH-7, or SNU-449 cells, 2×10^5 cells were collected in 100 μ L of PBS and incubated with 1 μ g of Cet-IR700 for 30 min at 4°C. To validate the specific binding of Cet-IR700, a 10-fold molar excess of unconjugated cetuximab was added 30 min before the incubation with Cet-IR700. Dead cells were excluded from the analysis based on the staining with Fixable Viability Dye. After washing with PBS, the fluorescence of the cells was analyzed by BD FACSLyric and FlowJo software.

2.6 | In vitro fluorescence microscopy

Hep3B, HuH-7, and SNU-449 cells were seeded at 1×10^4 on glass-bottomed dishes and incubated for 24 h. Cells were incubated with 100 μ L fresh culture medium containing 1 μ g Cet-IR700 for 1 h at 37°C and observed with a fluorescence microscope (IX81; Olympus America). Transmitted light differential interference contrast (DIC) images were obtained, and IR700 was detected using the filter set, which included a 608–668 nm excitation filter and a 672–712 nm bandpass emission filter. The cells were then exposed to NIR light (690 nm, 150 mW/cm², 50 J/cm²) using an ML7710 laser system (Modulight). The DIC images were acquired again 30 min after NIR light irradiation.

2.7 | In vitro NIR-PIT

Hep3B, HuH-7, SNU-449, or Ramos cells were seeded onto 24-well plates at 1×10^5 per well in quadruplicate in 1 mL medium. After

1 day, the cells were incubated with 5 μ g/mL of each APC for 1 h at 37°C. The cells were exposed to NIR light (690 nm, 150 mW/cm²) at 0, 1, 5, 10, 20, or 50 J/cm² using an ML7710 laser system (Modulight). After NIR-PIT, the cytotoxic effects of NIR-PIT with Cet-IR700 were determined by staining with Fixable Viability Dye. The percentage of unstained cells with Fixable Viability Dye was determined by BD FACSLyric flow cytometry and FlowJo software. For the assessment of ICD after NIR-PIT, we conducted evaluations on two ICD markers (calreticulin and Hsp70) as follows: Hep3B, HuH-7, and SNU-449 cells were seeded onto 24-well plates at 1×10^5 per well in quadruplicate in 1 mL medium. After 1 day, the cells were incubated with 5 μ g/mL of each APC for 1 h at 37°C. The cells were exposed to NIR light (690 nm, 150 mW/cm²) at 0 or 50 J/cm² using an ML7710 laser system. After NIR-PIT, cells were collected in 200 μ L PBS and incubated with PE-labeled anti-calreticulin (Polyclonal; Bioss), its PE-labeled rabbit IgG isotype control (Polyclonal; Bioss), PE-labeled anti-Hsp 70 Ab (Clone REA349; Miltenyi Biotec), and its PE-labeled human IgG1 isotype control (REA293; Miltenyi Biotec) which can detect compromised cell membranes for 30 min at 4°C. After washing with PBS, the fluorescence of the cells was analyzed by BD FACSLyric and FlowJo software. RFI was defined as the ratio of specific fluorescence (mean fluorescence of target cells incubated with the PE-labeled anti-calreticulin Ab or PE-labeled anti-Hsp70 Ab) over nonspecific fluorescence (mean fluorescence of target cells incubated with the PE-labeled rabbit IgG isotype control or PE-labeled human IgG1 isotype control).

2.8 | Animal and tumor model

All in vivo procedures were approved by the National Cancer Institute (NCI) Animal Care and Use Committee. Female homozygote athymic nude mice, 6–8 weeks old, were purchased from Charles River Laboratories. Hep3B (5.0×10^6) or HuH-7 (5.0×10^6) cells were inoculated into the right dorsum of mice. Mice with tumors reaching the diameter more than 4 mm were used for the experiments because the tumor in this subcutaneous model was initially flat and the volume could not be measured. Tumor volumes were evaluated three times per week using a tumor scanner (TumorImager2™; Bi-opticon) and calculated by TumorManager software. The mice were euthanized with inhalation of carbon dioxide gas when the tumor volume reached 800 mm³.

2.9 | In vivo EGFR expression analysis

Single-cell suspensions from Hep3B or HuH-7 tumor samples were prepared using the following protocol. Whole tumors were minced and incubated in RPMI medium containing collagenase type IV (cat. #LS004188, 1 mg/mL; Worthington Biochemical) and DNase I (cat. #11284932001, 20 μ g/mL; Millipore Sigma) at 37°C for 60 min, then gently cut with scissors, and physically dissociated with the back of the plunger of a 3 mL syringe. The tissues were

passed through a 70- μm cell strainer (Corning). Red blood cells (RBC) were removed by incubating with RBC lysis buffer (BioLegend). A total of 3.0×10^6 cells was stained, and data for 5.0×10^5 cells were collected for each tumor. The cells were stained with antibodies purchased from BioLegend (anti-CD31 [clone 390], anti-CD45 [clone 30-F11], and anti-PDPN [clone 8.1.1]) and Cell Signaling Technology (anti-EGFR [clone D1D4J] and Rabbit IgG isotype control [polyclonal]). Cells were also stained with fixable viability dye, and dead cells were gated out from the analysis. The fluorescence of the cells was then analyzed with the flow cytometer FACSLyric and FlowJo software. Tumor cells were determined as CD45-/CD31-/PDPN-. RFI was defined the same way as in vitro analysis.

2.10 | In vivo NIR-PIT

Tumor-bearing mice were randomized into three groups as follows: (i) no treatment (Control), (ii) intravenous injection of Cet-IR700 only (APC-IV), and (iii) intravenous injection of Cet-IR700 followed by NIR-PIT (NIR-PIT). Cet-IR700 (100 μg) was injected 12 and 10 days after Hep3B and HuH-7 cell inoculation, respectively (day 0). NIR laser light (690 nm, 150 mW/cm², 50 J/cm²) was administered to the tumor 24 h (day 1) and 48 h (day 2) after Cet-IR700 injection. Upon NIR light irradiation, a piece of aluminum foil with an aperture of approximately 1 cm diameter was placed over the mouse; then, the tumor was illuminated through the aperture to ensure that the NIR light was limited to the tumor site.

2.11 | Histological analysis

Tumor-bearing mice were randomized into the Control and NIR-PIT groups. For the NIR-PIT group, mice were exposed to NIR light (690 nm, 150 mW/cm², 50 J/cm²) 24 h after Cet-IR700 injection. To evaluate histological changes after NIR-PIT, tumors were harvested 24 h after NIR light irradiation. The formalin-fixed paraffin-embedded (FFPE) sections were prepared and stained with hematoxylin and eosin (H&E).

2.12 | Detection of DIG-labeled Ab by multiplex immunohistochemistry

Cetuximab or anti-human IgG1-Kappa isotype control (Abin vivo; 1 mg) was labeled with digoxigenin (DIG) by incubating 1 mg Ab and 50 μg DIG-NHS-ester (Thermo Fisher Scientific) using a similar method to IR700 conjugation. The resulting DIG-labeled Abs were abbreviated as cetuximab-DIG and isotype-DIG, respectively. Tumor-bearing mice were injected with cetuximab-DIG or isotype-DIG (100 μg) into the lateral tail vein. Tumors were harvested 24 h after injecting DIG-labeled Abs. The distribution of DIG-labeled Abs was analyzed in FFPE sections by multiplex

immunohistochemistry using anti-DIG Ab (clone 9H27L19; Thermo Fisher Scientific).

2.13 | Immunohistochemistry

Multiplex immunohistochemistry was carried out as described previously¹⁸ using an Opal Automation IHC Kit (Akoya Bioscience) and Bond RXm autostainer (Leica Biosystems). The sections were stained with DAPI and the following Abs: anti-CD45 (clone D3F8Q; Cell Signaling Technology; 1:500), anti-DIG (clone 9H27L19; Thermo Fisher Scientific; 1:500), anti-Ki-67 (clone D3B5; Cell Signaling Technology; 1:500), and anti-pCK (rabbit poly; Bioss Antibodies; 1:250). Stained slides were mounted with ProLong Diamond (Thermo Fisher Scientific) and imaged with a Mantra Quantitative Pathology Workstation (Akoya Biosystems). The obtained images were analyzed with inForm Tissue Finder software (Akoya Biosystems). To calculate the percentage of Ki-67 positive cancer cells, inForm software was trained to detect tissue and cell phenotypes using machine-learning algorithms based on the following criteria: areas with pCK expression = tumor, other areas = stroma, pCK+ CD45- cells = cancer cells, pCK- CD45+ = blood cells, and pCK- CD45- = other cells. inForm software computed the percentage of Ki-67-positive cells among cancer cells. The average percentage was calculated from five images for each specimen.

2.14 | Statistical analysis

Data are expressed as means \pm SEM. Statistical analyses were undertaken with GraphPad Prism (GraphPad Software). Associations between variables were tested with the Mann-Whitney U test. A one-way ANOVA followed by Tukey's test was used to compare multiple groups. For luciferase activity and tumor volumes, a repeated-measures two-way ANOVA followed by Tukey's test was used. $p < 0.05$ was considered significant.

3 | RESULTS

3.1 | Expression of EGFR in cell lines

Expression of EGFR on the surface of Hep3B, HuH-7, SNU-449, and Ramos cells was evaluated in vitro. EGFR was highly expressed in Hep3B, HuH-7, and SNU-449 cells, whereas no expression was detected in Ramos cells (Figure 1A). Next, to assess the binding of Cet-IR700 to Hep3B and HuH-7, and SNU-449 cells in vitro, they were incubated with Cet-IR700 and analyzed by flow cytometry. Hep3B, HuH-7, and SNU-449 cells showed a high IR700 fluorescence signal (Figure 1B). These signals were completely blocked by adding an excess of nonconjugated cetuximab (Figure 1B), indicating that Cet-IR700 binds explicitly to EGFR expressed on the surface of Hep3B, HuH-7, and SNU-449 cells.

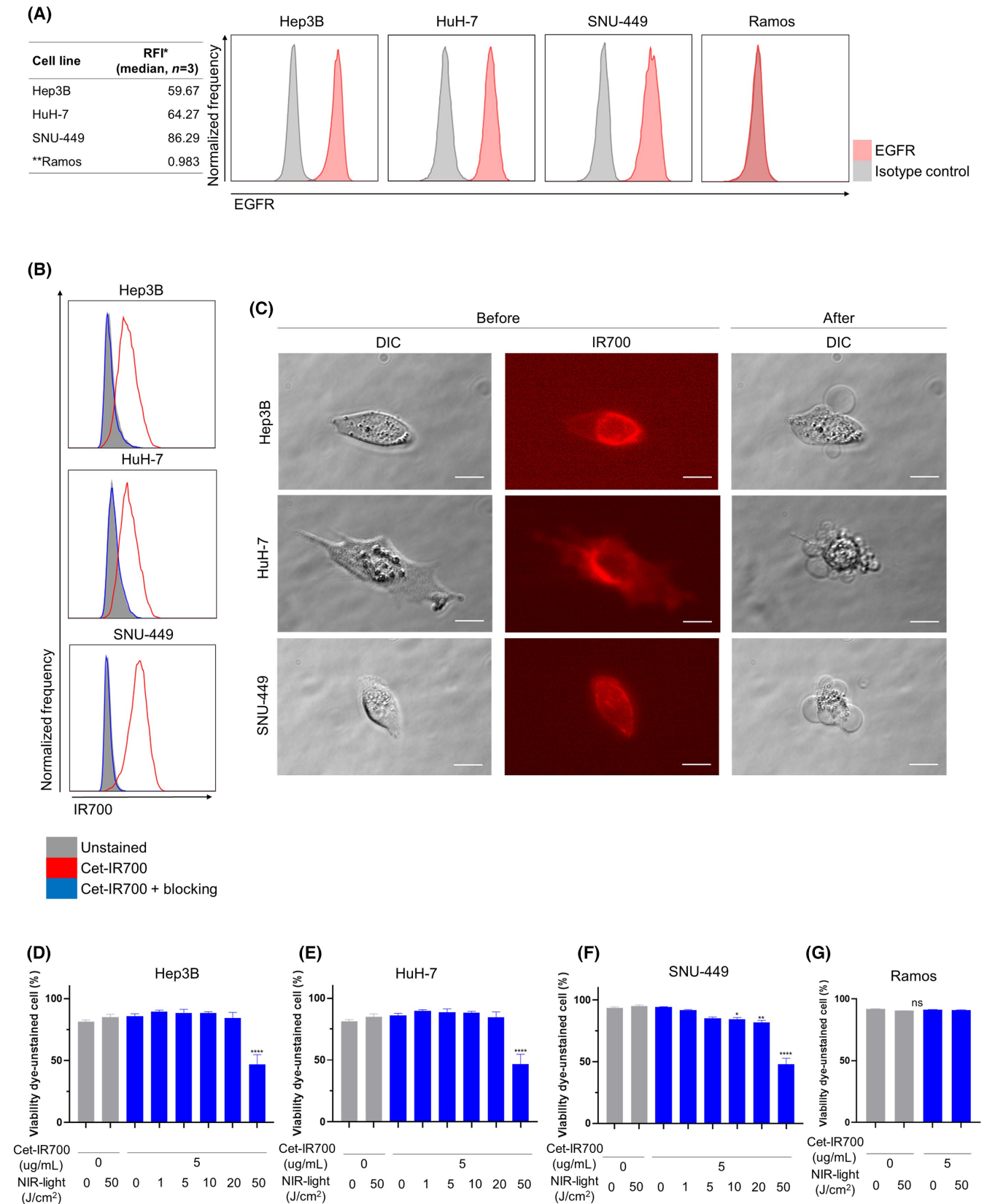


FIGURE 1 In vitro near-infrared photoimmunotherapy (NIR-PIT) using cetuximab-IR700 (Cet-IR700) in Hep3B, HuH-7, and SNU-449 cells. (A) Flow cytometric analysis of in vitro EGFR expression on Hep3B, HuH-7, SNU-449, and Ramos cells. RFI, relative fluorescence intensity. (B) Detection of Cet-IR700 bound to Hep3B, HuH-7, and SNU-449 cells by flow cytometric analysis. (C) Microscopic observation of cancer cells before and after in vitro NIR-PIT using Cet-IR700 (images, $\times 400$; scale bar, $20\ \mu\text{m}$). DIC, differential interference contrast. (D–G) Membrane damage of Hep3B (D), HuH-7 (E), SNU-449 (F), and Ramos (G) cells induced by in vitro NIR-PIT using Cet-IR700 was measured with Fixable Viability Dye ($n=4$; one-way ANOVA followed by Tukey's test). * $p < 0.05$. ** $p < 0.01$. *** $p < 0.0001$. ns, not significant versus untreated control.

3.2 | Target cell-killing efficacy of in vitro NIR-PIT using Cet-IR700

We evaluated the cell-killing efficacy of in vitro EGFR-targeted NIR-PIT using Hep3B, HuH-7, SNU-449, and Ramos cells. The cells were incubated with Cet-IR700, and cell morphology was microscopically examined after NIR light irradiation. In Hep3B, HuH-7, and SNU-449

cells, IR700 fluorescence was detected before NIR light irradiation, and cellular swelling was observed immediately after NIR light irradiation (Figure 1C). Cell membrane damage after in vitro NIR-PIT using Cet-IR700 was quantitatively evaluated using viability dye cytometric assay. The percentage of viability-unstained cells decreased after NIR-PIT in Hep3B, HuH-7, and SNU-449 cells in a light dose-dependent manner (Figure 1D-F). Treatment with Cet-IR700

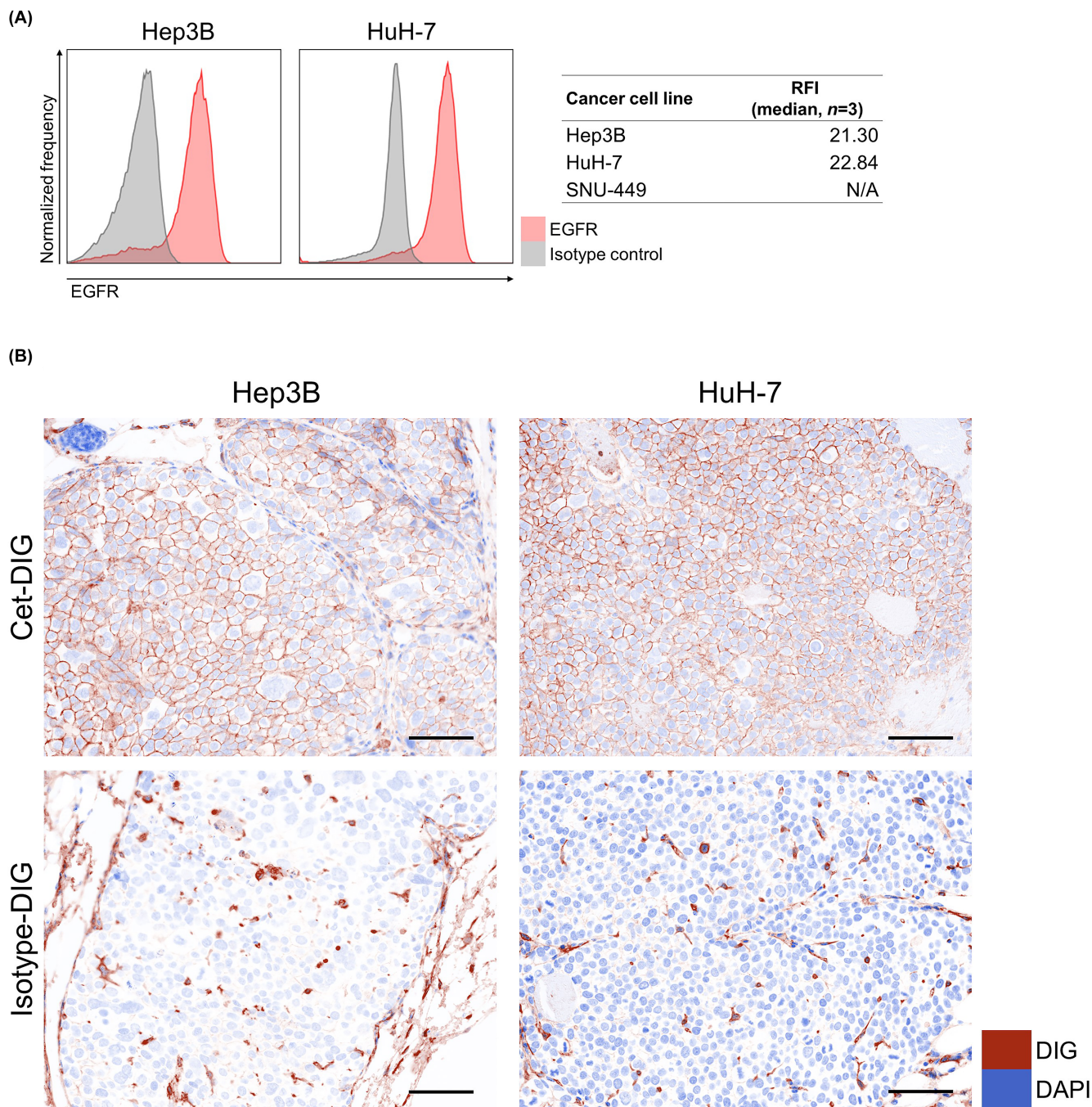


FIGURE 2 Expression of EGFR in cancer cells and delivery of cetuximab to Hep3B and HuH-7 cells in vivo. (A) Flow cytometric analysis of in vivo EGFR expression on Hep3B, HuH-7, and SNU-449 tumors ($n=3$). RFI, relative fluorescence intensity. N/A, not applicable. (B) Tumors were harvested 24h after injecting Cet-DIG or isotype-DIG into mice, and its distribution in Hep3B and HuH-7 was examined by multiplex immunohistochemistry (images, $\times 200$; scale bar, $100\mu\text{m}$). DAPI expression and DIG are shown in blue and brown, respectively. Cet-DIG, digoxigenin (DIG)-conjugated cetuximab.

alone or NIR light irradiation alone did not affect cell viability. However, NIR-PIT using Cet-IR700 did not damage Ramos cells with no EGFR expression (Figure 1G). In Hep3B, HuH-7, and SNU-449 cells, a significant increase in the expression of calreticulin and Hsp70 was observed after treatment (Figure S1).

3.3 | Expression of EGFR in cancer cells in vivo

We tested EGFR expression in established tumors of Hep3B and HuH-7. In the Hep3B and HuH-7 tumor model, the expression of EGFR in cancer cells was preserved (Figure 2A).

3.4 | Cet-IR700 delivery to cancer cells in vivo

To evaluate whether cetuximab was delivered to Hep3B and HuH-7 cells in vivo, either DIG-conjugated cetuximab (Cet-DIG) or isotype control (isotype-DIG) was infused into tumor-bearing mice, and then DIG distribution in the tumors was analyzed by multiplex immunohistochemistry. In Hep3B and HuH-7 tumors, Cet-DIG was detected on the cell surface (Figure 2B). Isotype-DIG was slightly detected in both tumors, which was likely to be mediated by Fc receptor binding. These results indicated that cetuximab was successfully delivered to the tumor tissue and bound to the surface of both Hep3B and HuH-7 cells.

3.5 | In vivo NIR-PIT using Cet-IR700 inhibits the growth of tumors

Therapeutic efficacy of in vivo NIR-PIT using Cet-IR700 was evaluated in Hep3B and HuH-7 tumor-bearing mice. Figure 3A shows the treatment and imaging schedule. Fluorescence imaging of IR700 is useful for evaluating the treatment efficacy because IR700 loses fluorescence upon NIR light irradiation. However, due to the highly

vascularized and dark nature of the tumor, it was not possible to evaluate fluorescent signal before and after NIR light irradiation using conventional methods.¹⁹ In the NIR-PIT group, the tumor size initially shrank after NIR light irradiation and then grew back over time; however, the growth was significantly slower than in the Control and APC-IV groups (Figure 3B,C).

3.6 | Histological changes after in vivo NIR-PIT using Cet-IR700

We examined the histology of the tumors 24 h after NIR-PIT to histologically evaluate the direct cytotoxic effects of in vivo NIR-PIT using Cet-IR700. On H&E staining, Hep3B and HuH-7 tumors showed large numbers of necrotic cells which typically showed fewer dark nuclei and eosinophilic cytoplasm with some vacuolar degeneration (Figure 4A). Such histological changes were not seen in the Control group. Next, we assessed Ki-67 expression among cancer cells to evaluate whether NIR-PIT exerted significant damage. In both tumors, the percentage of Ki-67-positive cancer cells was significantly lower in the NIR-PIT group compared with the Control group (Figure 4B,C).

4 | DISCUSSION

In the present study, we demonstrated that NIR-PIT using Cet-IR700 effectively killed HCC cells in vitro. EGFR was highly expressed on the surface of Hep3B and HuH-7 HCC tumor models, and Cet-IR700 bound strongly to these cells both in vitro and in vivo. NIR-PIT successfully inhibited tumor growth in both HCC xenograft models and substantially reduced Ki-67 positivity, denoting a reduction in cellular proliferation.

When considering the clinical application of NIR-PIT for HCC, it is important to consider potential side effects. Pharmacokinetically, cetuximab remains in the liver for several days.²⁰ Unbound APCs

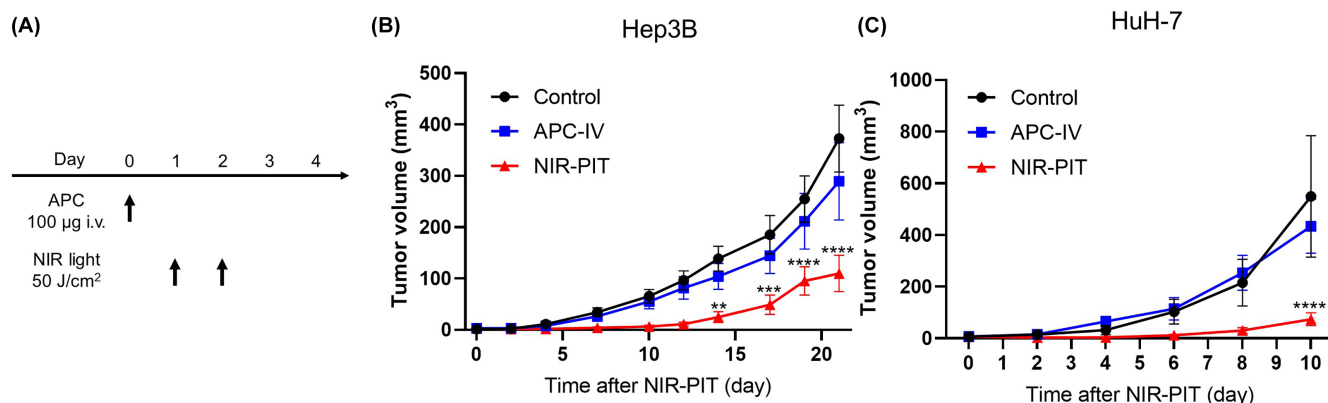


FIGURE 3 Efficacy of in vivo near-infrared photoimmunotherapy (NIR-PIT) using cetuximab-IR700 against Hep3B and HuH-7 tumors. (A) Treatment schedule. (B, C) Tumor volume curves in Hep3B (B) and HuH-7 tumors (C) ($n=8-9$; mean \pm SEM; repeated-measures two-way ANOVA followed by Tukey's test. ** $p < 0.01$; *** $p < 0.001$; **** $p < 0.0001$ versus control.)

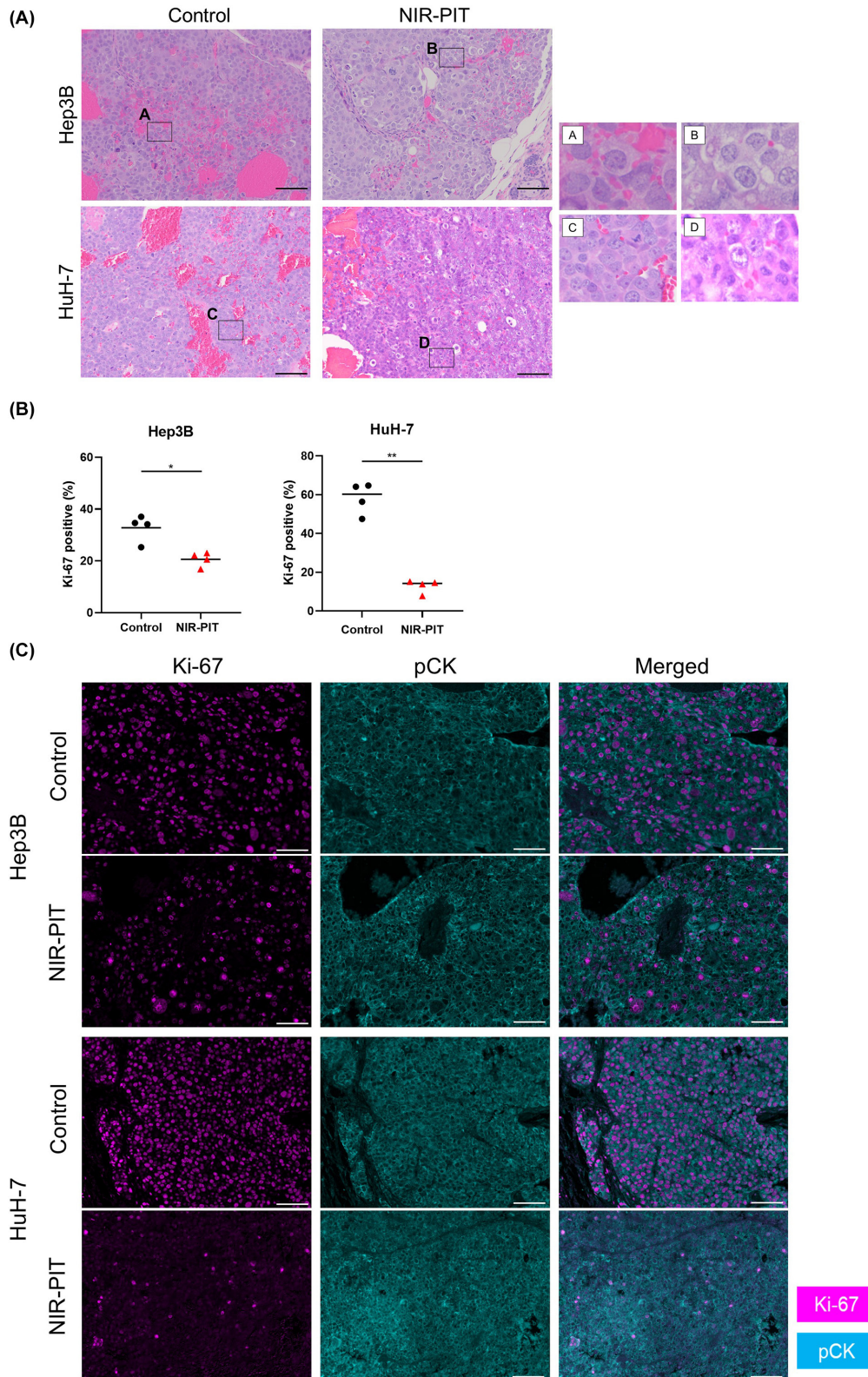


FIGURE 4 Histological changes after in vivo near-infrared photoimmunotherapy (NIR-PIT) using cetuximab-IR700. Tumor tissue histology was examined 24h after NIR-PIT. (A) H&E staining of Hep3B and HuH-7 tumors after NIR-PIT (images, $\times 200$; scale bar, $100\mu\text{m}$). Insets (A–D) are enlarged and displayed in the right panels. (B, C) Evaluation of Ki-67 positivity among cancer cells in Hep3B and HuH-7 tumors by multiplex immunohistochemistry. (B) Comparison of the percentage of Ki-67-positive cancer cells among two groups ($n=4$; the Mann Whitney U test). $*p < 0.05$; $**p < 0.01$. (C) Representative pictures of Ki-67 and pCK expression (images, $\times 200$; scale bar, $100\mu\text{m}$). Ki-67 and pCK expression is shown in magenta and cyan, respectively. pCK, pan-cytokeratin.

can generate reactive oxygen species upon exposure to NIR light irradiation under oxygen-rich conditions, leading to inflammation.²¹ However, the light dose can be constrained to the tumor using interstitial fiber optic catheters so that the normal liver does not receive much of the light. Indeed, the liver itself transmits NIR light relatively poorly due to high concentrations of hemoglobin and other chromophores²²; thus, we believe that it is technically feasible to selectively irradiate tumors with NIR light while minimizing damage to the hepatic parenchyma.

NIR-PIT using Cet-IR700, which has already been approved for clinical use and established to be safe for human use in head and neck cancers, has the potential to be a breakthrough in the treatment of HCC. Unlike other molecularly targeted drugs that require repeated administration, NIR-PIT with Cet-IR700 can be successful after only a single administration of the antibody in principle, making it both convenient and cost effective compared with other treatments. Also, NIR-PIT, which kills cancer cells specifically, is considered to be ideal for nonsurgical LDTs. LDTs such as radiofrequency ablation and transarterial chemoembolization are standard treatments for HCC and demonstrate excellent outcomes in early- and intermediate-stage HCC. However, a major drawback regarding treatment eligibility depends greatly on tumor size, location, and other patient factors such as platelet count. Specifically, these LDTs are ineffective against portal vein invasion and extrahepatic metastases. On the other hand, NIR-PIT has the potential to treat cases that cannot be addressed by these LDTs, as it can be used to treat any part of the body as long as NIR light can be delivered. Therefore, our treatment is not intended to supplant established treatment modalities but rather provide additional therapeutic options and perhaps complement existing modalities available for patients.

There are several limitations to this study. First, since we used human cell line-derived xenografts in immunodeficient mice, the effect of NIR-PIT on the anticancer immune activation could not be demonstrated. Such a study has to await the production of a suitable murine mAb against mouse EGFR that can be used in immunocompetent mouse tumor models. Nevertheless, we anticipate that EGFR-targeted NIR-PIT will activate the immune system as it has proven to be more effective in subjects with intact immune systems. Given that NIR-PIT results in ICD, we would anticipate a synergistic effect should this modality be combined with standard-of-care immune checkpoint blockade therapies. Additionally, long-term survival could not be assessed in this study because these subcutaneous HCC tumor models exhibited marked hypervascularization and fragility, leading to recurrent intratumoral hemorrhage. As a result, no significant differences in survival rates were observed within the NIR-PIT group in the present study because many animals had to be euthanized due to tumoral hemorrhage. However, tumor growth was suppressed in the NIR-PIT group, and a decrease in the expression of Ki-67, a prognostic factor for both disease-free survival and overall survival in HCC,²³ was observed. Therefore, we believe this study indicates that NIR-PIT using Cet-IR700 is a promising treatment for HCC.

In conclusion, we confirmed that EGFR is a promising selective target for HCC, which can be successfully exploited for NIR-PIT using Cet-IR700. Given that Cet-IR700 has demonstrated efficacy for patients with recurrent/refractory EGFR+ head and neck cancers, this agent could be explored in other EGFR+ malignancies, including HCC.

AUTHOR CONTRIBUTIONS

All authors read and approved the final version of the manuscript. ST mainly designed and conducted experiments, performed analysis, verified data, and wrote the manuscript. HF, TK, AF, SO, and KM performed experiments and analysis. AK and FEE identified and confirmed EGFR expression in HCC cell lines in vitro and in vivo, prepared the specimen, and evaluated the pathological findings. PLC wrote the manuscript and supervised the project. HK planned and initiated the project, designed and conducted experiments, verified data, wrote and edited the final manuscript, and supervised the entire project.

ACKNOWLEDGMENTS

This work was supported by the Intramural Research Program of the NIH, NCI, Center for Cancer Research (grant no. ZIA BC011513).

CONFLICT OF INTEREST STATEMENT

The authors have no conflict of interest.

ETHICS STATEMENT

Approval of the research protocol by an Institutional Reviewer Board: N/A.

Informed Consent: N/A.

Registry and the Registration No. of the study/trial: N/A.

Animal Studies: All in vivo procedures were carried out in compliance with the Guide for the Care and Use of Laboratory Animal Resources (1996), US National Research Council, and approved by the NCI Animal Care and Use Committee (MIP-003; project number P214396).

ORCID

Aki Furusawa  <https://orcid.org/0000-0002-1339-4219>

Hisataka Kobayashi  <https://orcid.org/0000-0003-1019-4112>

REFERENCES

1. Sung H, Ferlay J, Siegel RL, et al. Global cancer statistics 2020: GLOBOCAN estimates of incidence and mortality worldwide for 36 cancers in 185 countries. *CA Cancer J Clin.* 2021;71:209-249.
2. Farazi PA, DePinho RA. Hepatocellular carcinoma pathogenesis: from genes to environment. *Nat Rev Cancer.* 2006;6:674-687.
3. Hartke J, Johnson M, Ghabril M. The diagnosis and treatment of hepatocellular carcinoma. *Semin Diagn Pathol.* 2017;34:153-159.
4. Mitsunaga M, Ogawa M, Kosaka N, Rosenblum LT, Choyke PL, Kobayashi H. Cancer cell-selective in vivo near infrared photoimmunotherapy targeting specific membrane molecules. *Nat Med.* 2011;17:1685-1691.
5. Kobayashi H, Choyke PL. Near-infrared photoimmunotherapy of cancer. *Acc Chem Res.* 2019;52:2332-2339.

6. Sato K, Ando K, Okuyama S, et al. Photoinduced ligand release from a silicon phthalocyanine dye conjugated with monoclonal antibodies: a mechanism of cancer cell cytotoxicity after near-infrared photoimmunotherapy. *ACS Cent Sci*. 2018;4:1559-1569.
7. Ogata F, Nagaya T, Okuyama S, et al. Dynamic changes in the cell membrane on three dimensional low coherent quantitative phase microscopy (3D LC-QPM) after treatment with the near infrared photoimmunotherapy. *Oncotarget*. 2017;8:104295-104302.
8. Kira S, Nakanishi T, Suemori S, Kitamoto M, Watanabe Y, Kajiyama G. Expression of transforming growth factor alpha and epidermal growth factor receptor in human hepatocellular carcinoma. *Liver*. 1997;17:177-182.
9. Ito Y, Takeda T, Sakon M, et al. Expression and clinical significance of erb-B receptor family in hepatocellular carcinoma. *Br J Cancer*. 2001;84:1377-1383.
10. Kato T, Wakiyama H, Furusawa A, Choyke PL, Kobayashi H. Near infrared photoimmunotherapy; a review of targets for cancer therapy. *Cancer*. 2021;13:2535.
11. Berasain C, Avila MA. The EGFR signalling system in the liver: from hepatoprotection to hepatocarcinogenesis. *J Gastroenterol*. 2014;49:9-23.
12. Huether A, Hopfner M, Sutter AP, Schuppan D, Scherubl H. Erlotinib induces cell cycle arrest and apoptosis in hepatocellular cancer cells and enhances chemosensitivity towards cytostatics. *J Hepatol*. 2005;43:661-669.
13. Zandi R, Larsen AB, Andersen P, Stockhausen MT, Poulsen HS. Mechanisms for oncogenic activation of the epidermal growth factor receptor. *Cell Signal*. 2007;19:2013-2023.
14. Zhu AX, Stuart K, Blaszkowsky LS, et al. Phase 2 study of cetuximab in patients with advanced hepatocellular carcinoma. *Cancer*. 2007;110:581-589.
15. Zhu AX, Rosmorduc O, Evans TR, et al. SEARCH: a phase III, randomized, double-blind, placebo-controlled trial of sorafenib plus erlotinib in patients with advanced hepatocellular carcinoma. *J Clin Oncol*. 2015;33:559-566.
16. Jin H, Shi Y, Lv Y, et al. EGFR activation limits the response of liver cancer to lenvatinib. *Nature*. 2021;595:730-734.
17. Okada R, Kato T, Furusawa A, et al. Selection of antibody and light exposure regimens alters therapeutic effects of EGFR-targeted near-infrared photoimmunotherapy. *Cancer Immunol Immunother*. 2022;71:1877-1887.
18. Maruoka Y, Furusawa A, Okada R, et al. Interleukin-15 after near-infrared photoimmunotherapy (NIR-PIT) enhances T cell response against syngeneic mouse tumors. *Cancers (Basel)*. 2020;12:2575.
19. Fukushima H, Kato T, Furusawa A, et al. Intercellular adhesion molecule-1-targeted near-infrared photoimmunotherapy of triple-negative breast cancer. *Cancer Sci*. 2022;113:3180-3192.
20. Sato K, Watanabe R, Hanaoka H, et al. Photoimmunotherapy: comparative effectiveness of two monoclonal antibodies targeting the epidermal growth factor receptor. *Mol Oncol*. 2014;8:620-632.
21. Kato T, Okada R, Goto Y, et al. Electron donors rather than reactive oxygen species needed for therapeutic photochemical reaction of near-infrared photoimmunotherapy. *ACS Pharmacol Transl Sci*. 2021;4:1689-1701.
22. Stolik S, Delgado JA, Pérez A, Anasagasti L. Measurement of the penetration depths of red and near infrared light in human "ex vivo" tissues. *J Photochem Photobiol B*. 2000;57:90-93.
23. King KL, Hwang JJ, Chau GY, et al. Ki-67 expression as a prognostic marker in patients with hepatocellular carcinoma. *J Gastroenterol Hepatol*. 1998;13:273-279.

SUPPORTING INFORMATION

Additional supporting information can be found online in the Supporting Information section at the end of this article.

How to cite this article: Takao S, Fukushima H, King AP, et al. Near-infrared photoimmunotherapy in the models of hepatocellular carcinomas using cetuximab-IR700. *Cancer Sci*. 2023;114:4654-4663. doi:[10.1111/cas.15965](https://doi.org/10.1111/cas.15965)